The last gasps of massive stars life:

Silicon core burning, neutrino cooling, and core-collapse dynamics

Mathieu Renzo

April 6, 2024

Abstract

The core structure of massive stars determines the outcome of the following (non-hydrostatic) evolution, i.e. the outcome of the core-collapse and possible consequent supernova (SN) explosion. The SN successfully unbinds the stellar envelope, or fails, and the resulting compact object can be either a neutron star (NS) or a black hole (BH). Here, I describe the late phases of hydrostatic equilibrium during the the stellar life, namely silicon (Si) core burning, with particular attention to the nuclear and neutrino cooling processes, and discuss the present understanding of the core-collapse explosion dynamics.

Contents

1 Introduction

Massive stars can be defined as those that will end their life forming a compact object, either a neutron star (NS) or a black hole (BH). This requires them to consume (at least partially) the oxygen-rich core, that is, for the widest range of initial masses, to build a silicon-rich core and subsequently iron-rich core that is too massive to be sustained by the electron degeneracy pressure. This core is therefore doomed to collapse under the influence of its own self-gravity, and this can result in a successful supernova explosion. For single massive stars, this happens for initial mass $M_{\mathrm{ZAMS}} \gtrsim 7 - 10\,M_{\odot}$, depending on their metallicity and rotation rate [11]. The presence of companions, which is the rule rather than the exception [39], can also change this threshold [49].

While the surface properties of massive stars in late evolutionary stages are still uncertain (mostly because of uncertainties in their mass loss rate, [41, 37], see also Sec. 12.1

in [35]), the qualitative behavior of their cores is more established (in large part thanks to our knowledge of nuclear physics from laboratory experiments). After helium depletion, the core is made mainly of carbon and oxygen. These become the next nuclear fuel, with carbon igniting first[1]. Above the carbon-oxygen core, two shell sources exists burning helium and hydrogen, respectively. In low-mass stars, the ignition of the He shell in degenerate environment leads to "thermal pulses", ultimately removing the envelope and leading to the formation of a white dwarf. For massive stars, this does not happen since the He core is too hot to be degenerate.

During (late) carbon burning, a large fraction of the energy of the core is carried out by thermal neutrinos produced because of the high temperatures and densities reached [3] (see also Sec. 2.2). At this stage, neutrinos leave the star unimpeded (because of the inherently small cross sections for weak-interaction), which accelerates even further the evolution. This neutrino cooling becomes the dominant energy loss process in the late evolutionary stages (evolved massive stars are "neutrino stars" [14]).

After core carbon depletion, the star contracts and increasing further its temperature until it ignites neon (through photodisintegrations), and then oxygen, and finally silicon. Each fuel type is made of the ashes of the previous burning stages. For every new element processed in the core, a shell of the old type of fuel ignites above it, leading to the characteristic pre-SN onion-skin structure, see Fig. 1. However, the interplay between violent ignition episodes and mixing can smooth and merge boundaries between the various shells in ways that are not fully understood as of yet.

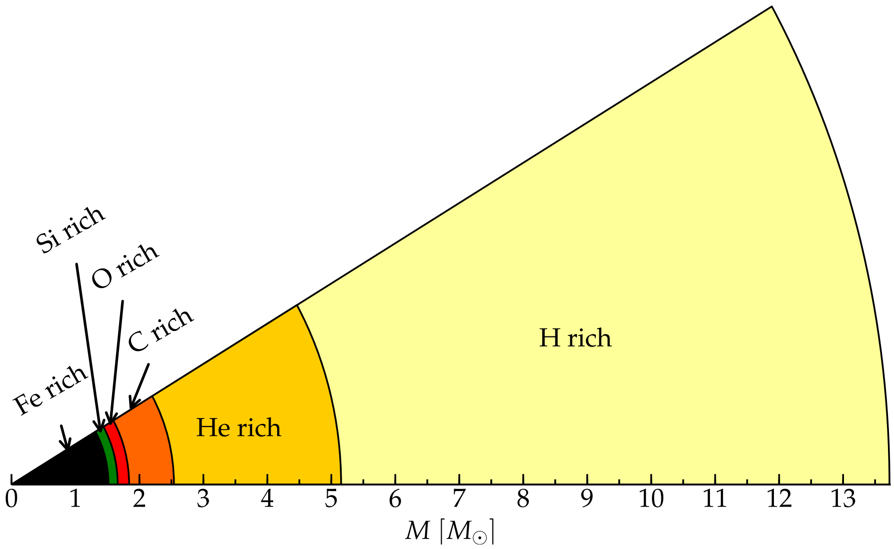

Fig. 1: Schematic structure of a single $15\,M_\odot$ star at the onset of core-collapse (see Eq. 6). The radius of each wedge is proportional to its mass. Note that the final mass is lower than $M_{\mathrm{ZAMS}}(= 15M_\odot)$ because of the wind mass loss. At the interface between each shell there is a nuclear burning region using the material of the overlying region as fuel. This is Fig. 1.2 of [36], from which significant portions of this document are taken.

The degenerate iron core is too massive to be sustained by the electron degeneracy pressure, and therefore it collapses because of gravity, reaches (super–)nuclear density ($\rho \sim 10^{14}$ g cm^{-3}), bounces due to the repulsive core of the nuclear force and this triggers a shock-wave. This shock wave is thought to explode the star, unbinding the stellar envelope. However, historically (hydrodynamical) simulations have had limited suc-

[1]Technically, carbon starts burning through the $^{12}\mathrm{C}(\alpha,\gamma)^{16}\mathrm{O}$ reaction which consumes α particles, i.e., before ^{4}He is depleted!

cess in producing explosions. In most cases, the shock just stops or reverts deep in the star. Therefore, a "shock–revival" mechanism (usually neutrino heating behind the shock aided by asymmetries in the flow) is needed to push it further and make it succeed in unbinding the stellar envelope.

The stellar structure (especially of the deepest layers) is paramount for the success or failure of the SN explosion, especially the density profile that the shock will encounter moving outward. But the details of the stellar structure depend on the late burning stages (namely, Si burning) of the star, and on the mixing processes during these phases.

Several attempts to define a (small set of) parameter(s) describing the pre-collapse core structure that could predict the outcome of the simulation of a SN explosion (success or failure, NS or BH remnant) have been made (e.g., [31, 12, 10]). Because the late burning phases and ultimately the formation of the collapsing core itself is a multi-physics, multi-scale, and likely stochastic problem, any attempt to define such a parameter is necessarily an attempt to average and (over?) simplify the structure [28].

2 Importance of the structure and composition of the iron core

The thermal state and composition of the iron core are of crucial importance for the collapse itself: a slight variation in one of these cause significant differences in the density profile of the star and can in principle influence the outcome of the evolution (i.e. successful explosion, or not). As an example, the amount of free electrons in the core, which is quantified by Y_e:

$$Y_e \stackrel{\text{def}}{=} \sum_i \frac{Z_i}{A_i} X_i \ , \tag{1}$$

enters quadratically in the effective Chandrasekhar mass,

$$M_{\text{Fe}} \geq M_{\text{Ch}}^{\text{eff}} \sim (5.83 M_\odot) Y_e^2 \left[1 + \left(\frac{s_e}{\pi Y_e} \right)^2 \right] \tag{2}$$

i.e. the maximum mass that can be sustained by electron degeneracy pressure.

The dynamics of the collapse, and therefore the success or failure of the explosion, depend on the structure (temperature, density, etc.) and details of the composition of the core.

2.1 Description of Silicon burning

Silicon burning produces as ashes all the elements of the so called "iron group"[2], and happens with central temperature and density between:

$$T \sim (3-5) \cdot 10^9 \ [\text{K}] \ , \ \rho \sim 10^7 - 10^{10} \ [\text{g cm}^{-3}] \tag{3}$$

This stage last only a few days, because the energy yield[3] of silicon burning is only of order 0.1 MeV nucleon^{-1} [1]. Consequently, the rates of the thermonuclear reactions must be very high in order to sustain the star, and the fuel is exhausted rapidly.

The nuclear reactions happening during Si burning proceed as follows. The nuclei which make the core (mainly Si) are photo-disintegrated

$$\gamma + {}^A Z \rightarrow {}^{A'} Z' + \{p, n, \alpha\} \ . \tag{4}$$

[2] Because the curves of abundances show a peak for the abundances of isotopes with $52 \lesssim A \lesssim 62$.
[3] cf. the hydrogen burning energy release is ~ 6.7 MeV nucleon^{-1}

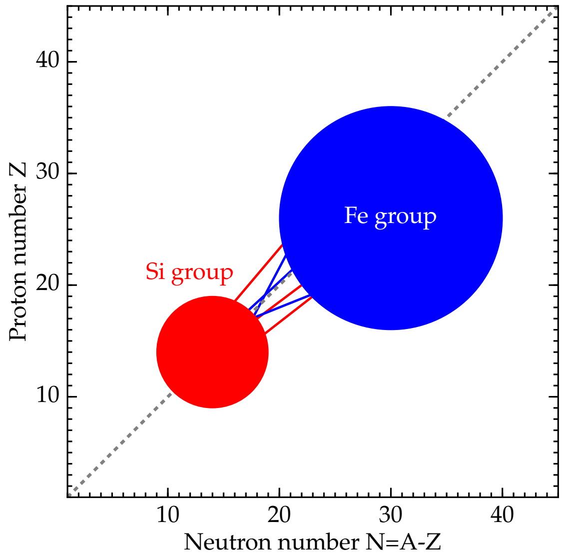

Fig. 2: Schematic representation of quasi statistical equilibrium on the nuclear chart. The two filled circle represent the Si (red) and Fe (blue) groups. The abundance of nuclei within each group reach NSE. The links connecting specific isotopes within each group represent the few reactions out of equilibrium, which progressively result in the depletion of the number of isotopes in the Si group in favor of those in the Fe group.

This produces light particles (i.e. protons, neutrons, αs), which are then captured by the remaining nuclei to build heavier (and unstable) nuclei of the iron group

$$\{p, n, \alpha\} + \{^{A}Z, ^{A'}Z'\} \rightarrow \{\text{Fe group nuclei}\} + \ldots \tag{5}$$

Moreover, many $^{A'}Z'$ nuclei produced by photo-disintegrations and particles captures are extremely neutron or proton rich, therefore a lot of weak reaction such as $\beta^{\pm}-$decays and electron captures[4] happen too. The weak reactions have a paramount role in the determination of the value of Y_e.

This process is computationally very challenging, since there are many forward and reverse reactions happening at very high rates but canceling each other out, resulting in a very *stiff* set of equations to solve for the evolution of the chemical composition. In this situation, the truncation errors in the floating point algebra of computers can easily become problematic. The rates are so high that the Quasi Statistical Equilibrium (QSE) regime is instaured: two distinct groups of isotopes in equilibrium are formed and only few reactions linking the two groups are out of balance with their reverse, see Fig. 2.

Within each "equilibrium group", the abundances of each isotope stay constant, because production and destruction reactions involving only isotopes of that group cancel out almost exactly. This means that within each group, Nuclear Statistical Equilibrium (NSE) is reached. To solve for the abundances within a NSE group, we can use the equivalent of a Saha equation for the nuclear scale (cf. ionization).

Note however that weak reaction are never balanced by their reverse reaction: the cross section for neutrino captures is too small at this stage. Strong and electromagnetic mediated nuclear reactions need to compensate also the weak reactions for the isotopes that can β-decay or capture electrons. Therefore this is not a true statistical equilibrium regime, and the "principle of detailed balance" does not hold strictly. Some widely used stellar evolution codes therefore do not rely on the approximation of "quasi equilibrium" and instead calculate directly all the reactions.

---

[4] Positron captures are always negligible for stars with $M_{\text{ZAMS}} \leq 40 M_{\odot}$[1].

2.2 Core Cooling

During evolutionary phases beyond He core depletion, the temperatures are so high that when the core is radiative, what carries away most of the energy is not the photon flux (the opacity is so high that the diffusion of radiation is rather slow), but instead the neutrino flux [3]. As the core evolves, it contracts and becomes increasingly hot and dense, consequently increasing its neutrino flux. For $T \gtrsim 5 \cdot 10^8$ K the neutrino carry away more energy than the photons, and stars whose interior reach such temperatures can be called "neutrino stars" [14]: $L_\nu \gg L_{\gamma,\ \mathrm{surf}}$. The neutrino emission from core C ignition onwards is an important contribution to the neutrino background of the Universe (comparable to the much shorter pulse of neutrinos produced at core-collapse). At Si core ignition, the neutrino flux is so high that we could detect the Si core ignition of Betelgeuse and prepare for its explosion!

These neutrinos are produced by 2 different kind of processes (see also Sec. 6.5 ans Sec. 12.3.1 of [35]):

- from nuclear reactions, such as $\beta^\pm-$decays or electron captures: these only reduce the energy generation of nuclear reaction, so they don't really cool the star, but they just decrease the energy release ($\varepsilon_{\mathrm{nuc}} \to \varepsilon_{\mathrm{nuc}} - \varepsilon_{\nu,\mathrm{nuc}}$). Particularly important for the late evolution of massive stars are neutrinos from the so-called URCA processes:

$$^{A}Z + e^- \to^{A} (Z-1) + \nu_e$$
$$^{A}(Z-1) \to^{A} Z + e^- + \bar{\nu}_e$$

  which produce one neutrino and one anti-neutrino without changing the composition of the star. This requires that the nucleus $^{A}(Z-1)$ is unstable to β^-−decay and the cross section for electron capture on ^{A}Z is non-negligible, which can happen during Si core burning and the subsequent collapse.

- thermal neutrinos from:

  plasmon processes $\gamma + \gamma_{pl} \to \nu_x + \bar{\nu}_x$,

  bremsstrahlung $e^- +^{A} Z \to e^- +^{A} Z + \nu_x + \bar{\nu}_x$,

  pair-production $\gamma + \gamma \to \nu_x + \bar{\nu}_x$,

  pair annihilation $e^+ + e^- \to \nu_x + \bar{\nu}_x$,

  photo-processes $\gamma + e^- \to e^- + \nu_x + \bar{\nu}_x$,

etc.. (see Fig.3b for some examples of Feynman graphs). These do not come from processes releasing energy, so they effectively carry away energy from the core and cool it (ε_ν is a negative contribution to $dL/dm = \varepsilon_{\mathrm{nuc}} + \varepsilon_g - |\varepsilon_\nu|$).

Note that the two categories of neutrinos have also quite different functional dependencies on the thermodynamical properties of the core. The nuclear neutrinos are mostly sensitive to the core temperature (except for pycno-nuclear reaction where the electron screening effectively makes the Coulomb barrier negligible), while neutrino cooling processes are mostly sensitive to the core density ρ. The typical energy carried away by neutrino-cooling processes is of the order of the thermal energy of the electrons (i.e., their Fermi energy if the region from where the neutrinos are emitted is partially degenerate, like it is typically the case during Si core burning).

Weak reaction have a key role in determining the duration of Si core burning, the amount of fuel effectively burned, and finally the temperature, structure and composition of the resulting iron core. In fact, if neutrino cooling is not efficient enough convection can start, increasing the amount of fuel available for Si burning. Moreover, efficient convection flattens the entropy in the core, changing significantly the density profile and potentially affecting the success or failure of the SN-explosion mechanism [43, 40].

3 Core Collapse

Since the nuclei of the iron group are the most tightly bound, the fusion of two of them would require energy input greater than the energy released. Therefore, inside the iron core, fusion reactions cannot compensate the energy loss of the star, and the core is doomed to collapse. The conventional definition for the onset of collapse [16] is

$$\max\{|v|\} \geq 10^3 \text{ km s}^{-1} \ , \tag{6}$$

where v is the radial infall velocity. The arbitrary threshold set by Eq. 6 is motivated by the fact that, at this point, the star is a few tenths of seconds (roughly a dynamical timescale) away from "core bounce" (see below). The central density is so high ($\rho \gtrsim 10^{10}$ g cm^{-3}) that stellar evolution codes usually cannot properly simulate the physics needed (e.g., the high density regions require a different equation of state - EOS, hydrostatic equilibrium does not hold any longer, neutrinos start to be trapped because of the higher density and neutrino opacity). However, this is a purely technical threshold, while in nature the evolution of such a star is continuous during collapse. Fig. 4 illustrates the velocity profile of a 15 $M_\odot$ star at the onset of core collapse.

During collapse, electron capture reactions, e.g.,

$$p + e^- \rightarrow n + \nu_e \ , \quad {}^A Z + e^- \rightarrow^A (Z-1) + \nu_e \ , \tag{7}$$

decrease Y_e, and diminishing $M_{\text{Ch}}^{\text{eff}}$ (see Eq. 2) accelerating the collapse further. Together with positron capture reactions, electron capture reactions form the so-called URCA processes, responsible for the lion's share of the cooling (provided by neutrinos) during the collapse phase. As the infall velocity progressively increases, the core divides into two separate parts [47]:

- **Inner Core**: in sonic contact and collapsing self-similarly (i.e. the infall velocity $|v| \propto r$). Its mass is given by:

  $$M_{\text{i.c.}} = \int_{|v(r)| \leq c_s(r)} 4\pi\rho(r) r^2 dr \ , \tag{8}$$

  where $c_s \equiv c_s(r)$ is the local sound speed, and the integral can be evaluated analytically[5]. The value of $M_{\text{i.c.}}$ at core bounce is almost independent of the stellar progenitor and it is about 1 $M_\odot$ [15, 48].

- **Outer Core**: in supersonic collapse, because at lower density the sound speed c_s decreases, so no information about the inner core can reach into the outer core.

The collapse goes on until the central density is so high ($\rho_c \sim 10^{14}$ g cm^{-3}) that the repulsive core of the nuclear force becomes relevant. This repulsive contribution causes a sudden stiffening of the EOS, and triggers the so-called core bounce, which is conventionally defined by an arbitrary threshold on the specific entropy at the edge of the inner core: $s = 3$ (in units of the Boltzmann constant k_b). The physical picture of the core bounce is the following. The inner core overshoots the equilibrium density of the stiffened EOS, stops collapsing and reverses its radial velocity. This launches a shock wave

[5] The dominant pressure term at high density ($\rho_c \gtrsim$ few $\times 10^9$ g cm^{-3}) is due to relativistic degenerated electrons, so we can take a polytropic EOS $P \propto \rho^{4/3}$ to evaluate $c_s = \sqrt{\partial P / \partial \rho}$.

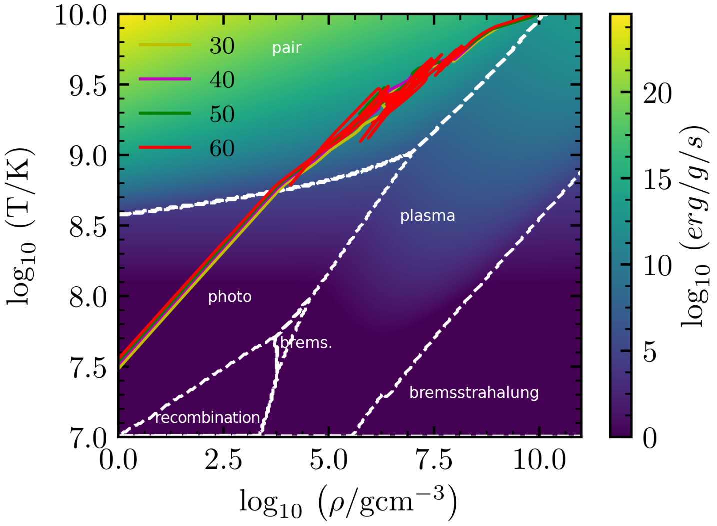

(a) ε_ν and stellar tracks on the temperature-density plane. White dashed lines indicate the regimes where different processes listed above dominate. Colored lines correspond to the evolutionary tracks of He cores of the mass indicated (in $M_\odot$ units). Credits: Rob Farmer, see also [20].

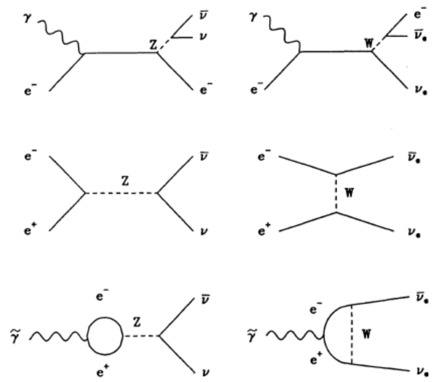

(b) Feynman diagrams for the dominant neutrino cooling processes. The top row shows the photo-emission processes, the middle row shows the $e^{\pm}$ annihilation processes, the bottom row shows the plasmon processes. The neutral (charged) current reactions are in the left (right) column. Fig. 1 in [3].

Fig. 3: Physics of neutrino cooling in stellar interiors

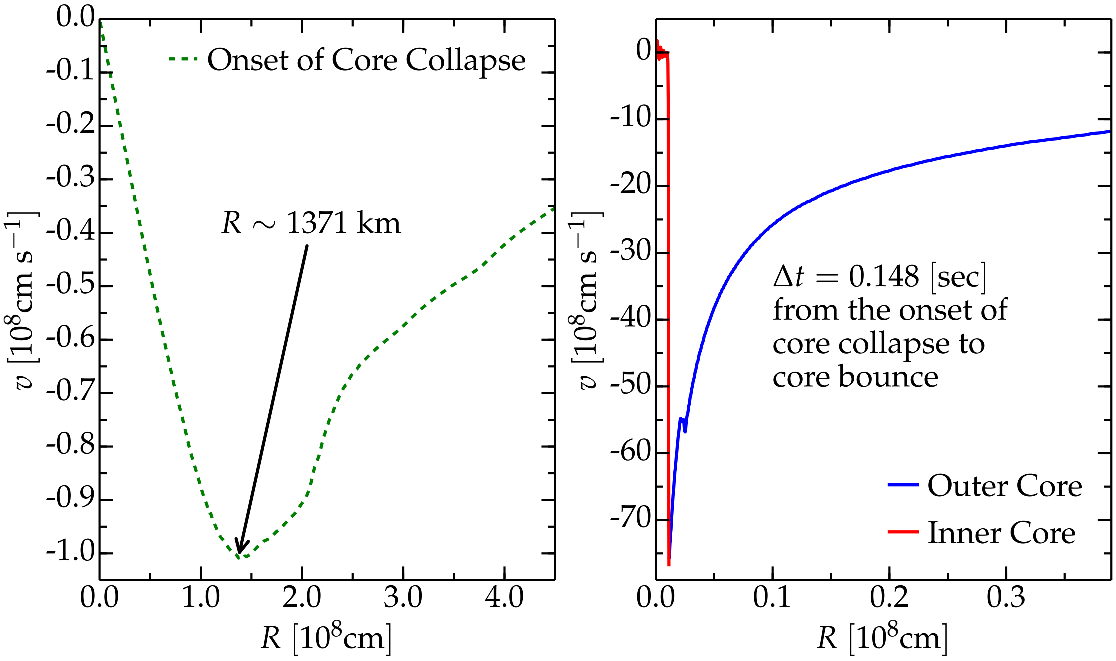

Fig. 4: Velocity profile for the core of an initially 15 $M_\odot$ star at the onset of core-collapse (left panel) and at core bounce (right panel). Note the linear behavior of the infall velocity in the inner core on the left panel. Note also the different scales on the two panels: at the onset of core collapse, the infall velocity is still subsonic and directed inward ($v < 0$) everywhere. The data in the right panel are obtained using the open-source code GR1D, [30], with the data at the onset of core collapse as input.

at the edge of the inner core. It is thought that this shock wave at least in some cases, successfully disrupts the star, producing a SN. However, in most cases, the shock needs to be "revived" by some mechanism.

The energy source to drive the explosion is the gravitational binding energy released by the collapse of $\sim 1.4\,M_\odot$ of Fe-rich material with radius of almost ~ 1000 km to a proto-NS with radius of ~ 10 km:

$$\Delta E_{\rm bind} \simeq \frac{GM^2}{R_{\rm NS}} - \frac{GM^2}{R_{\rm Fe}} \sim 10^{53}\,{\rm erg}\ , \tag{9}$$

The energy reservoir provided by the gravitational collapse is largely in excess of the total binding energy of the stellar envelope, and roughly speaking 100 times more that the typical kinetic energy of a SN explosions (1 Bethe $\equiv$ 1 f.o.e. $\equiv 10^{51}$ erg). Note that the energy radiated away by a SN is typically a small fraction of the kinetic energy ($\int L_{\rm SN}(t)\,dt \simeq 10^{49}$ erg).

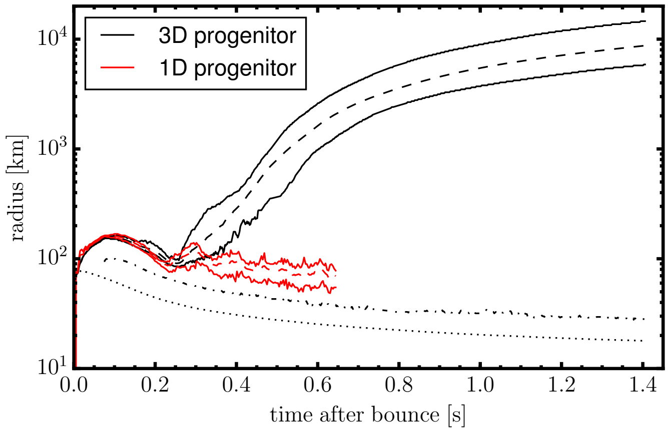

Fig. 5: Evolution of the minimum, maximum (solid lines), and average shock radius (dashed lines) for the explosion of an 18 $M_\odot$ stellar model. Red curves are computed in 1D: in spherical symmetry the shock stalls and its radius stays roughly constant. This is Fig. 5 of [27].

As the shock wave propagates in the outer core, it loses energy by heating and photodisintegrating the infalling material, and overcoming the ram pressure ($P_{\rm ram} \simeq \rho v^2$) of this same material. Moreover, all the neutrinos that are not absorbed in the "gain region" contribute to decreasing the total energy of the material behind the shock. The energy loss through these mechanisms leads to a stalled shock (the shock radius remains roughly constant for $\sim$ 0.1 millisec, see Fig. 5) in most simulations available to date. An uncertain "shock revival mechanism" must act to revive the shock and restart its radial expansion allowing it to unbind the stellar envelope and produce a SN explosion.

In the *neutrino driven paradigm* (for reviews see [23, 45]), the shock is pushed by the large neutrino emission from the hot proto-NS formed in the inner part of the bouncing inner core. These neutrinos are mostly produced by electron captures to "neutronize" the Fe core (in the innermost "cooling-region" where the proto-NS is), cf. Eq. 7 and from the cooling processes of Fig. 3b. A small fraction of these neutrinos will interact in a region behind the shock (the so-called "gain-region"). This is because the stellar plasma has now densities and temperatures higher than during core Si burning, and the cross section for neutrino absorption is not negligible anymore.

Note, however, that other explosion mechanism relying less heavily on the neutrino flux have been proposed. For instance, accretion on the forming compact object in the inner core might trigger energetic jets that might help pushing the shock, and this might be the dominant explosion mechanism for long gamma ray bursts and SNIc showing broad emission lines (i.e., very large ejecta velocities).

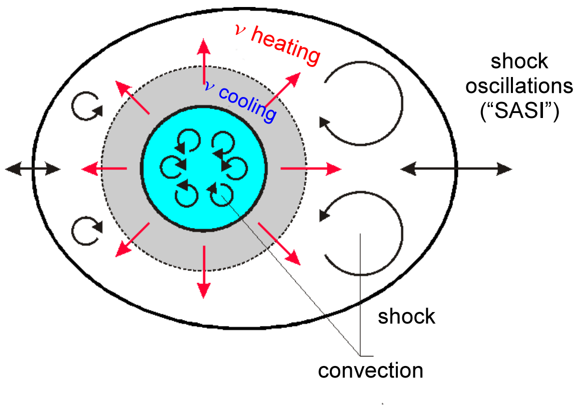

Fig. 6: Sketch of the key ingredients for a successful explosion in the neutrino driven paradigm, from [29].

3.1 Shock revival mechanisms

As mentioned above, historically, numerical simulations of core-collapse SNe would always find stalling and ultimately receding shocks, i.e. failed explosions. This lead to the realization that the *asymmetries* in the flow are a key ingredient to achieve a successful explosion.

Several sources of asymmetry (both local and global) exist in the collapsing core of a massive star, most are summarized in Fig. 6:

- The neutrino heat the bottom of the gain region, driving convection (a steep temperature and entropy gradient can develop because of the neutrino heating);
- Convection implies the presence of turbulent flow and an associated turbulent pressure ($P_{\rm turb} \simeq \rho v_{\rm turb}^2$) that can help pushing the shock [32],
- Standing accretion Shock Instability (SASI, [6]): when the shock stalls its surface is perturbed by the infalling material. These perturbation (e.g., in terms of the local velocity) are advected downwards by convection and amplified which leads to a sloshing motion of the shock[6]
- Lepton Emission Self-Sustained Emission (LESA, [44]), found in 3D simulations where the neutrino emission is roughly dipolar.

The overall effect of asymmetries is to (i) increase the amount of time spent by matter in the gain region, where the energy of the neutrinos can be harvested and used to push the shock (ii) provide extra pressure terms (e.g., due to turbulence). The combination of these two should result, at least in some cases, in successful explosions.

The first axisymmetric (i.e., 2D) simulations showed some successful explosion, but it was soon realized that the symmetry imposed artificially in these calculation (cf. Fig. 7) was changing the turbulent cascade: instead of dripping towards smaller scale and be dissipated at the viscous scale, energy is pumped to larger scales in 2D, which artificially helps the explosion.

As of early 2019, there is an emerging picture from the 3D core-collapse SN simulations of different research groups ([34, 25]): *not only the asymmetries during the first millisecond after core-bounce are necessary to achieve successful explosions, but also the pre-collapse core-structure and in particular the Si/O interface is crucial.*

The most massive stellar cores, for which the Si/O interface is at a large Lagrangian mass coordinate, develop strong neutrino driven convection, which together with the

[6]The growth time of this instability may be too long for it to play a role in successful explosions, where other mechanism revive the shock faster than SASI can develop [7].

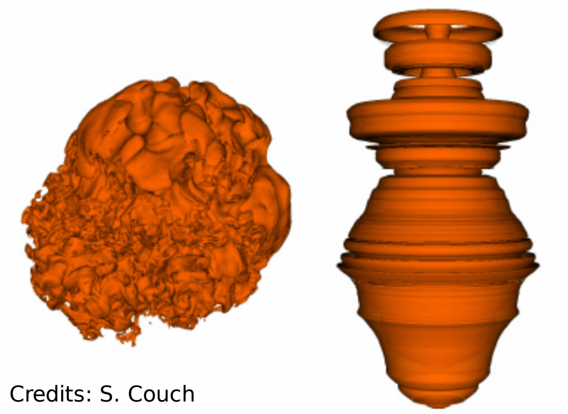

Fig. 7: Visualization of the shock morphology in 3D (left) and 2D (right): clearly the artificial imposition of a symmetry by running at lower dimensionality changes the dynamics of the explosion.

contribution of the turbulent pressure drives a successful explosion with significant fall-back and result in the formation of a black hole.

Intermediate mass cores show a steep density gradient at the Si/O interface: if the shock can reach this interface, it will significantly accelerate outwards (because of mass continuity and the drop in the impinging ram pressure). The neutrino driven convection and turbulent pressure combined with the density drop result in successful explosions with neutron star remnant. Smaller cores show strong SASI oscillations of the shock and delayed explosions, likely also resulting in NS remnants. However, note that the landscape on explosion physics in the literature is itself very dynamic, with multiple groups working on this problem and disagreeing on the details.

Note that here we have not mentioned *rotation* and *magnetic fields*. These may play an important role in the explosion mechanism – certainly in relatively more rare explosions such as long gamma-ray bursts, and possibly for any explosion producing $\gtrsim 10^{52}$ erg of energy.
These are also very active research topics, where our understanding of the progenitor structure (in terms of angular momentum and magnetic fields) is even more uncertain.

3.2 Supernova kicks

The current understanding of core-collapse dynamics suggests that asymmetries are likely the key to the success of the explosion. This is further confirmed by the large velocities at which we observe some single NSs moving. The proper motion of radio pulsars can correspond to velocities in excess of $\sim$1000 km s^{-1}, which is much higher than the maximum velocity at which we observe O and B type stars moving.

These are explained invoking an energy and momentum re-distribution between the forming compact object and the SN ejecta allowed by the asymmetries. One possible source of asymmetry is if the neutrino flux from the cooling region is itself non-spherical, however, since the proto-NS that occupies most of the volume of the cooling region is convective with a convective turnover timescale faster than the explosion, this explaination is currently disfavored. Another possibility is that hydrodynamical instabilities lead to aspherical flows.

Whether the SN shock achieves a runaway radial growth (successful explosion, cf. black lines in Fig. 5) or it stalls and reverts (failed explosion, likely to result in BH formation) is typically decided within the first few 100 millisec after core-bounce. However, until few seconds after core-bounce the deeper layers of the ejecta and the proto-NS are still dynamically connected, and interact through gravity [21, 8]. If a clump of ejecta is more dense because of asymmetries in the flow (a situation routinely realized in 3D ab-initio simulations of the core-collapse process), it can gravitationally pull the newly born compact object in its direction and accelerate it.

A key prediction of this "tug-boat" model is that the SN shock is faster in the direction opposite to the one in which the compact object is accelerated. A faster shock is more efficient at photodisintegrating nuclei, producing light particles that can be accreted by the surviving nuclei: this model predicts stronger explosive nucleosynthesis in the direction opposite to the compact object. This prediction seems to be consistent with observations of supernova remnant for which we can find the associated NS [18, 24]. Note however, that recent simulations from [8] disagree with this picture, and produce sizable natal kicks just through momentum conservation in asymmetric ejecta.

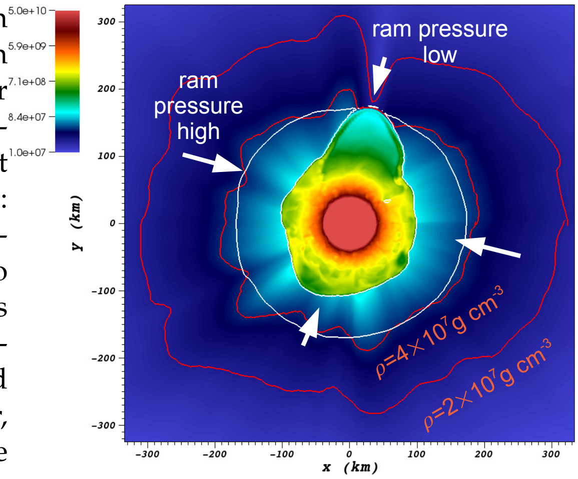

Fig. 8: Schematic of the development of a large asymmetry in a 3D CCSN simulation resulting in a large natal kick. From [29].

Because of the SN kick, the kinetic energy of the compact object is greatly increased, and this can lead to an increase of the total (orbital) energy of a putative binary system:

$$E_{\mathrm{orb}} = \frac{1}{2}M_1 v_1^2 + \frac{1}{2}M_2 v_2^2 - \frac{GM_1M_2}{a} \overset{\mathrm{SN}}{\rightarrow} \frac{1}{2}(M_1 - M_{\mathrm{ej}})(v_1 + v_{\mathrm{kick}})^2 + \frac{1}{2}M_2 v_2^2 - \frac{GM_1M_2}{a} > 0 \tag{10}$$

where we implicitly assume an instantaneous explosion (compared to the orbital period of the binary), which leaves the gravitational interaction term unchanged. If E_{orb} becomes positive, the binary system is unbound. The SN kick thus breaks most massive binary systems by giving a large velocity to the compact object, but without modifying significantly the instantaneous velocity of the companion star[7]

$$v_2 = \frac{M_1}{M_1 + M_2} v_{\mathrm{orb}} \equiv \frac{M_1}{M_1 + M_2}\sqrt{\frac{G(M_1 + M_2)}{a}} \ . \tag{11}$$

The companion star is thus shot out of the binary with its pre-explosion v_2, and if $v_2 > 30\,\mathrm{km\,s^{-1}}$ it becomes a runaway star [38]. This however tends to happen rarely, since mass transfer during the binary evolution tends to increase the separation a, decrease the mass M_1, and increase the mass M_2.

Note typically SN ejecta achieve velocities of $10\,000\,\mathrm{km\,s^{-1}} \gg v_{\mathrm{orb}}$, thus we can neglect the orbital motion of the binary during the SN (although see also [4]): effectively this corresponds to an instantaneous loss of mass from the exploding star, which is not the center of mass of the binary. This off-center mass loss (from the point of view of the binary) is also referred to as or "Blaauw kick" and can modify the orbit, and in extreme case where $M_{\mathrm{ejecta}} \geq (M_1 + M_2)/2$ it can change it from an circle/ellipse to a parabola/hyperbole - so unbind the binary [5]. Typically in massive binary evolution, the exploding star loses its H-rich envelope to the companion long before its SN explosion, therefore M_{ej} is rarely sufficiently large to unbind the binary without a natal kick due to asymmetries.

[7] Do not confuse v_2 with the orbital velocity $v_{\mathrm{orb}} = \sqrt{\frac{G(M_1+M_2)}{a}}$ which represents the velocity of the point of reduced mass μ orbiting around the center of mass of the binary, and not the velocity of a physical object!

From the observation of the pulsars proper motions we know that at least some NS receive such large kicks, however there is still debate on whether SN resulting in the formation of a BH can also provide significant kicks, and consequently whether most BHs remain bound to their stellar companion, or whether their formation breaks the binaries in which they form. In at least a handful of cases, it can be shown that large mass BHs were formed with negligible natal kicks [46].

The observation of double pulsars [19] also raises the question of whether some successful SN explosion resulting in NS formation might also lead to systematically smaller kicks, allowing for a binary to survive two consequent explosions. The idea is that ultra-stripped SNe (i.e. the explosion of a star that has lost a very substantial amount of mass in multiple binary mass transfer episodes), and/or electron-capture SNe[8] or core-collapse SN of small Fe cores would more easily result in a successful explosion (no shock stalling, and no time to develop significant asymmetries during a shock stalling phase) with consequently small kicks.

4 The Supernova Zoo

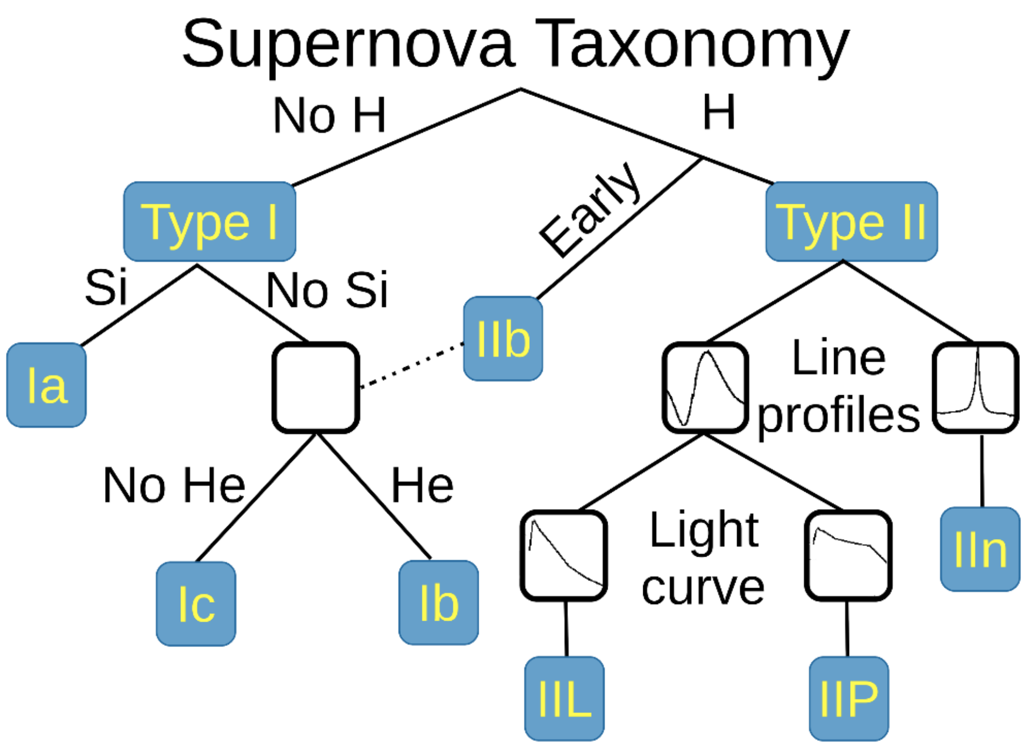

Fig. 9: Schematic representation of the SN taxonomy, based on spectral features and light curve shape. This figure is inspired by Fig. 2 in [9]. The dot-dashed line indicates the possible connection between SN events detected in late stages and classified as type Ib/Ic and SNe of type IIb.

As described in §3, the presumable final fate of a massive star is a core-collapse SN. The observational classification of a core-collapse SN depends on the spectrum and light curve it produces (e.g. [9] and references therein). The connection between the stellar progenitor and the resulting SN (if there is a successful explosion) is a topic of active

[8]The least massive stars to explode might never become hot enough to burn completely the oxygen core, leaving a partially degenerate oxygen-neon-magnesium composition. As this core contracts and cools through neutrino emission, it reaches densities sufficient to trigger electron capture on the nuclei of the core, decreasing the electron degeneracy pressure support and triggering the core-collapse.

research. For the sake of completeness, I report here the schematic classifications of all SN types, including also those that do not involve core-collapse, see Fig. 9.

It is worth underlining that the SN classification is to a great extent historic and does not always match the physics of the progenitor star and of the explosion. The first distinction between SN-types is based on the presence of hydrogen lines in the spectrum: the SNe showing no hydrogen are classified as type I SNe, while those with hydrogen are classified as type II SNe.

Type I SNe are further subdivided based on the presence of other elemental lines. Those showing silicon lines are type Ia SNe, and the proposed progenitor is *not* a massive star, but instead a white dwarf (WD) that experiences a thermonuclear explosion triggered by merger or mass accretion. In this scenario, the explosion happens only when a certain threshold condition is met, explaining the homogeneity in the luminosity decay and spectral features of the objects in this class (however, see [9] and references therein for further discussion). Type I SNe without silicon lines are further divided into those showing helium lines (type Ib), and those without helium lines (type Ic). These type Ib/Ic are thought to be the outcome of the collapse of a massive star that has lost all or most of its envelope either to stellar winds or a binary companion.

The subdivision of type II SNe is instead based on the shape and flux of the lines (mostly Hα): the presence of narrow emission lines classifies the SN event as a type IIn (where "n" stands for narrow). These are usually very bright SNe, and the theorized progenitor is a massive star producing a core-collapse explosion shock wave running into a dense circumstellar material (CSM). If the spectrum does not show narrow lines, then the sub-classification is based on the light curves, in particular the behavior of the luminosity decay. If the magnitude decays linearly in time (i.e. exponential decay of the luminosity), then the SN is classified as a type IIL. Instead, if there is a phase of constant luminosity (i.e. a "plateau"), the SN is classified as a type IIP. Finally, if the spectrum shows only temporarily some weak hydrogen lines, the SN is classified as a type IIb (because of the analogy with a type Ib/Ic SN). Other sub-categories keep on being defined as we explore the time-domain astronomy with deeper and higher cadence surveys.

Except type Ia SN, all other types are thought to be the outcome of a core collapse event (e.g. [9] and references therein). The differences among core-collapse SNe are strongly correlated with the structure and (outer) composition of the progenitor, and the presence of a dense circumstellar material (CSM). Mass loss has an important role in shaping both the CSM and the outer portion of the SN-progenitor structures and compositions, and thus its observational manifestation [37].

Further readings

- Asymmetric core-collapse as gravitational wave sources [33]
- Review on massive stars evolution [26]
- Supernova kicks [22, 21]
- Observation of supernovae [13, 42]
- Thermonuclear explosions of white-dwarfs [2, 17]

References

[1] W. D. Arnett. Advanced evolution of massive stars. VII - Silicon burning. *Astrophys. J. Supp. Ser.*, 35:145, October 1977.

[2] W. D. Arnett. Type I supernovae. I - Analytic solutions for the early part of the light curve. *Astrophys. J.*, 253:785–797, February 1982.

[3] M. B. Aufderheide. Convection and neutrino emission in the late stages of massive star evolution. *Astrophys. J.*, 411:813, July 1993.

[4] A. Batta, E. Ramirez-Ruiz, and C. Fryer. The Formation of Rapidly Rotating Black Holes in High-mass X-Ray Binaries. *Astrophys. J. Lett.*, 846:L15, September 2017.

[5] A. Blaauw. On the origin of the O- and B-type stars with high velocities (the "run-away" stars), and some related problems. *Bull. Astr. Neth.*, 15:265, May 1961.

[6] J. M. Blondin, A. Mezzacappa, and C. DeMarino. Stability of Standing Accretion Shocks, with an Eye toward Core-Collapse Supernovae. *Astrophys. J.*, 584:971–980, February 2003.

[7] Adam Burrows, David Vartanyan, and Tianshu Wang. Black Hole Formation Accompanied by the Supernova Explosion of a 40 $M_\odot$ Progenitor Star. *Astrophys. J.*, 957(2):68, November 2023.

[8] Adam Burrows, Tianshu Wang, David Vartanyan, and Matthew S. B. Coleman. A Theory for Neutron Star and Black Hole Kicks and Induced Spins. *arXiv e-prints*, page arXiv:2311.12109, November 2023.

[9] E. Cappellaro and M. Turatto. Supernova Types and Rates. *Invited review at the meeting: "The influence of binaries on stellar population studies", ed. D. Vanbeveren (Brussels 21-25 Aug. 2000)*, 2000.

[10] S. M. Couch, M. L. Warren, and E. P. O'Connor. Simulating Turbulence-aided Neutrino-driven Core-collapse Supernova Explosions in One Dimension. *arXiv:1902.01340*, February 2019.

[11] Carolyn L. Doherty, Pilar Gil-Pons, Lionel Siess, and John C. Lattanzio. Super-AGB Stars and their Role as Electron Capture Supernova Progenitors. *PASA*, 34:e056, November 2017.

[12] T. Ertl, H.-T. Janka, S. E. Woosley, T. Sukhbold, and M. Ugliano. A Two-parameter Criterion for Classifying the Explodability of Massive Stars by the Neutrino-driven Mechanism. *Astrophys. J.*, 818:124, February 2016.

[13] A. V. Filippenko. Optical Spectra of Supernovae. *Ann. Rev. Astron. Astroph.*, 35:309–355, 1997.

[14] G. S. Fraley. Supernovae Explosions Induced by Pair-Production Instability. *Astrophys. Space Sci.*, 2:96–114, August 1968.

[15] P. Goldreich and S. V. Weber. Homologously collapsing stellar cores. *Astrophys. J.*, 238:991, June 1980.

[16] A. Heger, S. E. Woosley, and H. C. Spruit. Presupernova Evolution of Differentially Rotating Massive Stars Including Magnetic Fields. *Astrophys. J.*, 626:350, June 2005.

[17] Wolfgang Hillebrandt and Jens C. Niemeyer. Type IA Supernova Explosion Models. *Ann. Rev. Astron. Astroph.*, 38:191–230, January 2000.

[18] T. Holland-Ashford, L. A. Lopez, K. Auchettl, T. Temim, and E. Ramirez-Ruiz. Comparing Neutron Star Kicks to Supernova Remnant Asymmetries. *Astrophys. J.*, 844:84, July 2017.

[19] R. A. Hulse and J. H. Taylor. Discovery of a pulsar in a binary system. *Astrophys. J. Lett.*, 195:L51–L53, January 1975.

[20] N. Itoh, H. Hayashi, A. Nishikawa, and Y. Kohyama. Neutrino Energy Loss in Stellar Interiors. VII. Pair, Photo-, Plasma, Bremsstrahlung, and Recombination Neutrino Processes. *Astrophys. J. Supp. Ser.*, 102:411, February 1996.

[21] H.-T. Janka. Natal kicks of stellar mass black holes by asymmetric mass ejection in fallback supernovae. *Mon. Not. Roy. Astron. Soc.*, 434:1355–1361, September 2013.

[22] H.-T. Janka. Neutron Star Kicks by the Gravitational Tug-boat Mechanism in Asymmetric Supernova Explosions: Progenitor and Explosion Dependence. *Astrophys. J.*, 837:84, March 2017.

[23] Hans-Thomas Janka. Explosion Mechanisms of Core-Collapse Supernovae. *Annual Review of Nuclear and Particle Science*, 62(1):407–451, November 2012.

[24] S. Katsuda, M. Morii, H.-T. Janka, A. Wongwathanarat, K. Nakamura, K. Kotake, K. Mori, E. Müller, T. Takiwaki, M. Tanaka, N. Tominaga, and H. Tsunemi. Intermediate-mass Elements in Young Supernova Remnants Reveal Neutron Star Kicks by Asymmetric Explosions. *Astrophys. J.*, 856:18, March 2018.

[25] T. Kuroda, K. Kotake, T. Takiwaki, and F.-K. Thielemann. A full general relativistic neutrino radiation-hydrodynamics simulation of a collapsing very massive star and the formation of a black hole. *ArXiv:1801.01293*, January 2018.

[26] N. Langer. Presupernova Evolution of Massive Single and Binary Stars. *Ann. Rev. Astron. Astroph.*, 50:107, September 2012.

[27] B. Müller. The Status of Multi-Dimensional Core-Collapse Supernova Models. *PASA*, 33:e048, September 2016.

[28] B. Müller. A Critical Assessment of Turbulence Models for 1D Core-Collapse Supernova Simulations. *arXiv:1902.04270*, February 2019.

[29] Bernhard Müller. The Core-Collapse Supernova Explosion Mechanism. In J. J. Eldridge, J. C. Bray, L. A. S. McClelland, and L. Xiao, editors, *The Lives and Death-Throes of Massive Stars*, volume 329 of *IAU Symposium*, pages 17–24, Nov 2017.

[30] E. O'Connor and C. D. Ott. A new open-source code for spherically symmetric stellar collapse to neutron stars and black holes. *Classical and Quantum Gravity*, 27(11):114103, June 2010.

[31] E. O'Connor and C. D. Ott. Black Hole Formation in Failing Core-Collapse Supernovae. *Astrophys. J.*, 730:70, April 2011.

[32] Evan P. O'Connor and Sean M. Couch. Exploring Fundamentally Three-dimensional Phenomena in

High-fidelity Simulations of Core-collapse Supernovae. *Astrophys. J.*, 865:81, Oct 2018.

[33] C. D Ott. TOPICAL REVIEW: The gravitational-wave signature of core-collapse supernovae. *Classical and Quantum Gravity*, 26(6):063001, March 2009.

[34] C. D. Ott, L. F. Roberts, A. da Silva Schneider, J. M. Fedrow, R. Haas, and E. Schnetter. The Progenitor Dependence of Core-collapse Supernovae from Three-dimensional Simulations with Progenitor Models of 12–40 $M_\odot$. *Astrophys. J. Lett.*, 855:L3, March 2018.

[35] O Pols. *Stars*. https://etd.adm.unipi.it/t/etd-05062015-125630/.

[36] M. Renzo. Systematic Study of Mass Loss in the Evolution of Massive Stars. Master's thesis, Università di Pisa, Italy, 2015. https://etd.adm.unipi.it/t/etd-05062015-125630/.

[37] M. Renzo, C. D. Ott, S. N. Shore, and S. E. de Mink. Systematic survey of the effects of wind mass loss algorithms on the evolution of single massive stars. *Astron. Astrophys.*, 603:A118, July 2017.

[38] M. Renzo, E. Zapartas, S. E. de Mink, Y. Götberg, S. Justham, R. J. Farmer, R. G. Izzard, S. Toonen, and H. Sana. Massive runaway and walkaway stars. A study of the kinematical imprints of the physical processes governing the evolution and explosion of their binary progenitors. *Astron. Astrophys.*, 624:A66, April 2019.

[39] H. Sana, S. E. de Mink, A. de Koter, N. Langer, C. J. Evans, M. Gieles, E. Gosset, R. G. Izzard, J.-B. Le Bouquin, and F. R. N. Schneider. Binary Interaction Dominates the Evolution of Massive Stars. *Science*, 337:444, July 2012.

[40] Fabian R. N. Schneider, Philipp Podsiadlowski, and Eva Laplace. Bimodal Black Hole Mass Distribution and Chirp Masses of Binary Black Hole Mergers. *Astrophys. J. Lett.*, 950(2):L9, June 2023.

[41] N. Smith. Mass Loss: Its Effect on the Evolution and Fate of High-Mass Stars. *Ann. Rev. Astron. Astroph.*, 52:487, August 2014.

[42] Nathan Smith, Weidong Li, Alexei V. Filippenko, and Ryan Chornock. Observed fractions of core-collapse supernova types and initial masses of their single and binary progenitor stars. *Mon. Not. Roy. Astron. Soc.*, 412(3):1522–1538, April 2011.

[43] T. Sukhbold and S. E. Woosley. The Compactness of Presupernova Stellar Cores. *Astrophys. J.*, 783:10, March 2014.

[44] I. Tamborra, F. Hanke, H.-T. Janka, B. Müller, G. G. Raffelt, and A. Marek. Self-sustained Asymmetry of Lepton-number Emission: A New Phenomenon during the Supernova Shock-accretion Phase in Three Dimensions. *Astrophys. J.*, 792:96, Sep 2014.

[45] David Vartanyan, Matthew S. B. Coleman, and Adam Burrows. The collapse and three-dimensional explosion of three-dimensional massive-star supernova progenitor models. *Mon. Not. Roy. Astron. Soc.*, 510(4):4689–4705, March 2022.

[46] Alejandro Vigna-Gómez, Reinhold Willcox, Irene Tamborra, Ilya Mandel, Mathieu Renzo, Tom Wagg, Hans-Thomas Janka, Daniel Kresse, Julia Bodensteiner, and Tomer Shenar. Observational evidence for neutrino natal kicks from black-hole binary VFTS 243. *arXiv e-prints*, page arXiv:2310.01509, October 2023.

[47] S. E. Woosley, A. Heger, and T. A. Weaver. The evolution and explosion of massive stars. *Reviews of Modern Physics*, 74:1015, November 2002.

[48] A. Yahil and J. M. Lattimer. Supernovae for pedestrians. In M. J. Rees and R. J. Stoneham, editors, *NATO Advanced Science Institutes (ASI) Series C*, volume 90 of *NATO Advanced Science Institutes (ASI) Series C*, pages 53–70, November 1982.

[49] E. Zapartas, S. E. de Mink, R. G. Izzard, S.-C. Yoon, C. Badenes, Y. Götberg, A. de Koter, C. J. Neijssel, M. Renzo, A. Schootemeijer, and T. S. Shrotriya. Delay-time distribution of core-collapse supernovae with late events resulting from binary interaction. *Astron. Astrophys.*, 601:A29, May 2017.